

Paper-based immunosensor utilizing dielectrophoretic trapping of microprobes for quantitative and label free detection using electrochemical impedance spectroscopy

Muhammad Omar Shaikh, Lung-Yu Chang, Cheng-Ho Chen, Ting-Feng Wu, and Cheng-Hsin Chuang

Citation: [Biomicrofluidics](#) **12**, 064102 (2018); doi: 10.1063/1.5057731

View online: <https://doi.org/10.1063/1.5057731>

View Table of Contents: <http://aip.scitation.org/toc/bmf/12/6>

Published by the [American Institute of Physics](#)



Don't let your writing
keep you from getting
published!

AIP | Author Services

Learn more today!

Paper-based immunosensor utilizing dielectrophoretic trapping of microprobes for quantitative and label free detection using electrochemical impedance spectroscopy

Muhammad Omar Shaikh,¹ Lung-Yu Chang,² Cheng-Ho Chen,³
Ting-Feng Wu,⁴ and Cheng-Hsin Chuang^{1,a)}

¹*Institute of Medical Science and Technology, National Sun Yat-sen University, Kaohsiung, Taiwan*

²*Department of Mechanical Engineering, Southern Taiwan University of Science and Technology, Tainan, Taiwan*

³*Department of Chemical and Material Engineering, Southern Taiwan University of Science and Technology, Tainan, Taiwan*

⁴*Department of Biotechnology, Southern Taiwan University of Science and Technology, Tainan, Taiwan*

(Received 15 September 2018; accepted 5 November 2018; published online 13 November 2018)

In this study, we have developed a novel paper based immunoassay for the quantitative detection of immunoreactions using electrochemical impedance spectroscopy. Paper provides an attractive platform for fabrication of simple, low cost, and portable diagnostic devices as it allows passive liquid transport, is biocompatible, and has tunable properties such as hydrophilicity, flexibility, permeability, and reactivity. We have used screen-printing to fabricate interdigitated electrodes (finger width and gap of 200 μm) on the paper substrate, while UV-lithography enables patterning of the paper into hydrophobic/hydrophilic regions. As a proof of concept, we have used this immunosensor to detect the immune response of Human Serum Albumin (HSA) antibody-antigen complex formation. To enable efficient immobilization of HSA antibodies, we have utilized dielectrophoresis to trap microprobes (MPs) on the electrode surface. The microprobes consist of an alumina nanoparticle core with a well-adhered polyaniline outer coating to which the HSA antibodies are conjugated in an oriented manner via covalent chemistry. The efficacy of the impedance-based immunosensor is compared when MPs are immobilized specifically on the electrode surface using dielectrophoresis (DEP) as opposed to being dropped and immobilized via physical absorption on the entire sensing area. Results show that a more reproducible and sensitive response is observed when DEP is utilized to trap the microprobes. Furthermore, the normalized impedance variation during immunosensing shows a linear dependence on the concentration of HSA with an observed limit of detection of 50 $\mu\text{g}/\text{ml}$, which is lower than conventionally used paper based urine dipsticks used for urinary protein detection. Thus, we have developed a low cost paper based immunoassay platform that can be used for the quantitative point of care detection of a wide range of immunoreactions. *Published by AIP Publishing.* <https://doi.org/10.1063/1.5057731>

I. INTRODUCTION

To enable effective public health monitoring, especially in the developing world, diagnostic tests must fulfill certain criteria which include being affordable, easy to use, portable, and able to operate with little or no external equipment. Paper based biosensors have emerged as an alternative technology for fabricating low cost diagnostic devices, especially for resource limited settings.

^{a)}Author to whom correspondence should be addressed: chchuang@imst.nsysu.edu.tw. Tel.: +886 7 5252000 ext. 5785.

Besides the fact that paper is inexpensive and widely available in a range of formats, it has certain properties that make it an attractive platform for biosensing applications. These include (i) the ability to wick fluids via capillary action without the need for an external pumping system; (ii) patterning of paper into hydrophobic/hydrophilic regions and fabricating 3-dimensional assays by stacking or folding paper;¹⁻³ (3) the biocompatibility and porosity of paper enables safe storage of reagents; (4) the lightweight and flexibility of paper in addition to the ease of safe disposal via combustion make it a highly suitable platform for single-use tests. The use of paper for fabrication of analytical devices and its application for low cost point of care testing has already been demonstrated. The most common examples of paper-based assays include urinalysis test strips for simultaneous detection of various analytes including protein and glucose and immunochromatographic lateral flow assays (LFAs) such as home pregnancy tests. While the potential of paper for effective calorimetric detection has been demonstrated,^{4,5} there are still opportunities for fabricating paper based diagnostic devices that utilize other modes of detection, particularly electrical/electrochemical detection, while still retaining low cost and simplicity.

The ability to perform electrochemical detection on paper should enable the fabrication of paper based immunosensors that provide quantitative analysis as opposed to currently used calorimetric assays that are either semi-quantitative or simply give a yes/no response. Immunosensors have been widely employed for several applications including healthcare because they can achieve rapid and sensitive detection of the specific binding of an antigen to its corresponding antibody to form a stable complex.^{6,7} Immunosensors utilizing electrochemical detection are insensitive to color contamination and can be effectively integrated with the miniaturized hardware, making them arguably the most practical and quantifiable diagnostic technique for detection of proteins.⁸⁻¹⁰ The fabrication of paper-based immunosensors utilizing electrochemical detection requires electrode integration on the paper substrate that is achieved using several methods among which cost-effective printing protocols like screen¹¹ or inkjet¹² printing are most commonly used. Generally, inks made of carbon based materials (graphite or nanomaterials like graphene) and metals like gold, platinum, or silver are good choices for fabricating working and counter electrodes while the reference electrode, if utilized, is generally made of the Ag/AgCl paste.

Among the various electrochemical techniques, impedance based electrical transduction, where the applied electrical signal is alternating as opposed to direct, can be used to analyze both the resistive and the capacitive changes at the electrode surface over a wide frequency range during immunosensing. This analytical approach, known as electrochemical impedance spectroscopy (EIS), is an effective strategy for probing of complex bio-recognition events¹³ and has been utilized in a wide range of biosensors ranging from bacteria and pathogen detection to immunosensing and DNA characterization.¹⁴⁻¹⁶ EIS can be used for real time and direct monitoring of affinity binding events without the need for labeling compounds. To fabricate a sensitive paper based impedimetric immunosensor, it is crucial that the receptor antibody is selectively immobilized on the electrode surface.

The proposed paper based immunosensor utilizes dielectrophoresis (DEP) to trap antibody-conjugated microprobes on interdigitated microelectrodes printed using screen-printing. Furthermore, the efficacy of the immunosensor has been compared when the microprobes are trapped on the electrode surface using DEP as opposed to being dropped on the surface and immobilized via physical absorption. DEP is a versatile technique that has been used for controllable, selective, and accurate manipulation of a wide variety of bioreceptors onto the surface of the electrode sensing platform.¹⁷ DEP is defined as the time-averaged force acting on a spherical dielectric particle immersed in a medium and exposed to a spatially non-uniform electric field.¹⁸ The magnitude and direction of this force are dependent on the electric field intensity, particle size, and permittivity and on the conductivity of the particle and the suspension medium. In our previous works, we have utilized programmable three step DEP manipulation to effectively distinguish bladder cancer staging using multiple biomarkers on a single glass based lab on a chip device.¹⁹ Microelectrodes, in comparison to conventional electrodes, significantly improve sensitivity, especially in low conductivity solutions, and allow rapid reaction kinetics with an improved signal to noise ratio.²⁰ We have chosen an interdigitated electrode design because the fabrication protocol is simpler and the geometry enables improved sensitivity over other microelectrode designs.

Furthermore, the conventionally used three electrode design for performing electrochemical measurements has limitations for use in paper as the printed Ag/AgCl reference electrode is unable to maintain a stable potential in the absence of high concentration of chloride ions in solution. To the best of our knowledge, this is the first proof-of-concept paper based immunosensor utilizing DEP for impedance-based detection.

II. EXPERIMENTAL

A. Microprobe synthesis

In this study, we have utilized micrometer-sized probes or microprobes (MPs), which consist of conductive polyaniline (PANI) coated alumina nanoparticles (Al_2O_3 NPs) conjugated to HSA antibodies, and are referred to as $\text{Al}_2\text{O}_3/\text{PANI}/\text{Ab-HSA}$ MPs. The conjugation of antibodies with nanoparticles has been widely utilized for developing immunosensors as it combines the novel intrinsic properties of nanoparticles and their enhanced surface areas with the selective and specific recognition capabilities of antibodies to antigens. While the dielectric Al_2O_3 NP core enables effective manipulation using DEP, the polyaniline coating provides a conductive channel to the electrodes and allows for oriented conjugation of antibodies via covalent chemistry.

1. Surface modification of Al_2O_3 NPs

We have utilized a surface modification technique where dodecyl benzene sulfonic acid (DBSA) was used to obtain a uniform and well-adhered PANI coating on the alumina nanoparticles. Functional protonic acids like DBSA absorb most of the aniline monomers onto their complex network as their long aliphatic chains facilitate efficient mixing while their long hydrocarbon tail allows for easy modification of the polymer-polymer interface.²¹ To obtain the coating, 3 g of aniline monomer, 8.4115 g of DBSA, 7.35 g of ammonium persulfate (APS), and 2 g of Al_2O_3 NPs (~20 nm) were used. First, the Al_2O_3 NPs were added to the aniline solution and ultrasonicated for 10 min, followed by the addition of the DBSA solution, and further sonication for 10 min. The APS solution was then added and the system was allowed to react for 2 h. The PANI was polymerized by standard oxidative polymerization of the aniline monomer in the presence of APS as the oxidizing agent. Following polymerization, the dark green $\text{Al}_2\text{O}_3/\text{PANI}$ microparticle (MP) was filtered, washed multiple times with DI water using centrifugation, and baked in an oven at 60 °C for 30 min to obtain $\text{Al}_2\text{O}_3/\text{PANI}$ MPs in the dry powdered form.

The morphology of the Al_2O_3 NPs before and after they are surface modified with the PANI coating can be observed in the FE-SEM images shown in Fig. 1(a). It can be seen that the modified $\text{Al}_2\text{O}_3/\text{PANI}$ microparticles have an irregular and coalesced surface appearance that is markedly different from the powdered Al_2O_3 NPs. TEM images in Fig. 1(b) show that the PANI surface modification promotes aggregation and cluster formation of the Al_2O_3 NPs, resulting in sizes in the micrometer range. Furthermore, we have performed a FTIR analysis to confirm the presence of the PANI coating. The peaks appearing at 1562 cm^{-1} and 1484 cm^{-1} can be assigned to the C–C stretching modes of quinoid and benzenoid rings, respectively, while the characteristic peak (circled in green) at 3440 cm^{-1} corresponds to the N–H stretch of amine groups present in PANI as shown in Fig. 1(c). The band at about 1382 cm^{-1} can be assigned to the C–N stretching vibrations. The strong peak at 1124 cm^{-1} corresponds to C–H bending vibrations based on the degree of electron delocalization and hence is a characteristic of PANI conductivity. These findings are consistent with previously reported works^{22,23} and the $\text{Al}_2\text{O}_3/\text{PANI}$ MPs can thus be used as antibody carriers in our immunosensor.

2. Antibody conjugation

We have used a simple and effective protocol to conjugate the HSA antibodies to the $\text{Al}_2\text{O}_3/\text{PANI}$ MPs as schematically illustrated in Fig. 2(a). First, the antibodies are oxidized in a solution containing 1 mM of sodium metaperiodate and 0.1M sodium acetate with the pH maintained at 5.5. This step causes the oxidation of the carbohydrate moieties present in the heavy chain of the

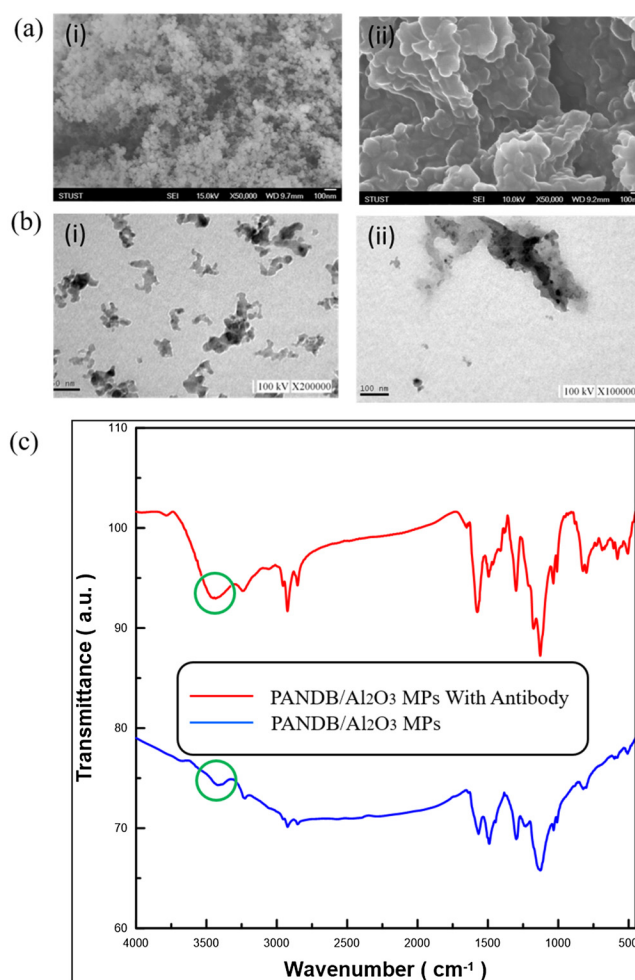


FIG. 1. (a) FE-SEM and (b) TEM images of Al₂O₃ NPs (i) before and (i) after surface modification with PANI (scale bar corresponds to 100 nm). (c) FTIR spectra of the Al₂O₃/PANI MPs (blue) and after conjugation with HSA (red).

antibody and results in the formation of aldehyde groups. Next, Al₂O₃/PANI NPs are added to the oxidized antibody solution and mixed under constant rotational stirring at room temperature for 30 min. During this step, the aldehyde groups of the oxidized antibodies covalently bind with the amino groups of PANI present in the surface modified Al₂O₃ NPs through the formation of an amide bond. This covalent interaction allows oriented conjugation where the fragment crystallizable region (Fc) of the antibody is bound to the nanoparticle surface while the fragment antigen-binding region (Fab) is available during immunoassay. The synthesized Al₂O₃/PANI/ab-HSA MPs are collected by centrifugation at 18 000 rpm for 5 min, dispersed in DI water, and stored at 4 °C until further use. We have also performed optical density analysis using a spectrophotometer to study conjugation efficiency of HSA antibodies to the Al₂O₃/PANI MPs. A 97.8% reduction in optical density of the supernatant before and after conjugation with HSA antibody as shown in Fig. 2(b) confirms that conjugation was successful.

B. Immunosensor fabrication and operation

The fabrication of the paper-based immunosensor can be primarily categorized into three stages: (i) Screen printing of interdigitated electrodes (IDEs); (ii) Patterning of paper into hydrophobic/hydrophilic regions using ultraviolet (UV) lithography; (iii) Immobilization of microprobes, which are deposited either directly on the entire sensing area or specifically trapped on the IDEs

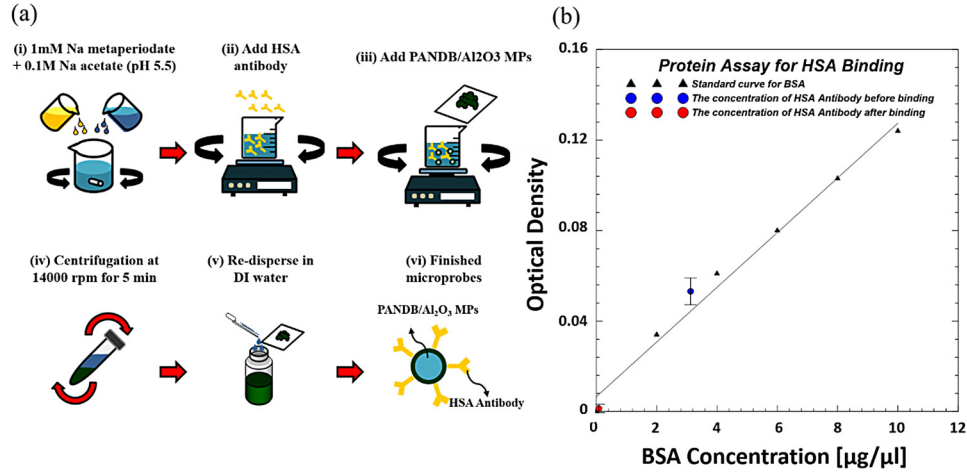


FIG. 2. (a) The step-by-step fabrication protocol for HSA conjugation to $\text{Al}_2\text{O}_3/\text{PANI}$ MPs. (b) Optical density analysis confirms successful conjugation.

using positive-dielectrophoresis (p-DEP). The step-by-step fabrication protocol is schematically illustrated in Fig. 3(a). The IDEs are printed on the filter paper (Advantec Grade no: 4a, pore size $1\ \mu\text{m}$) using a screen printer (SYP-4570, Ag PRO Technology Corporation, Taiwan) operating at a speed of 100 mm/s. Screen printing allows transfer of the microparticulate silver ink onto the paper substrate except in areas that are made impermeable by the use of a blocking stencil. The printed IDE has 8 fingers with each finger having a width and interspacing of $200\ \mu\text{m}$, respectively, resulting in a total sensing area of $37.2\ \text{mm}^2$. The thickness of the filter paper was 0.2 mm and the depth of the ink penetration as seen in the cross sectional image in Fig. 3(b) was about 0.1 mm. After screen printing, the electrodes are thermally cured in an oven at 150°C for 30 min to remove organic solvents present in the ink and sinter the silver microparticles for improved physical and electrical properties. Next, the paper is patterned into hydrophobic/hydrophilic regions using UV-lithography where the sensing areas and the IDE lead regions remain hydrophilic, while the rest of the sensor is hydrophobic. First, UV-curable resin (U54-0, HICO Technology Co., LTD.) is

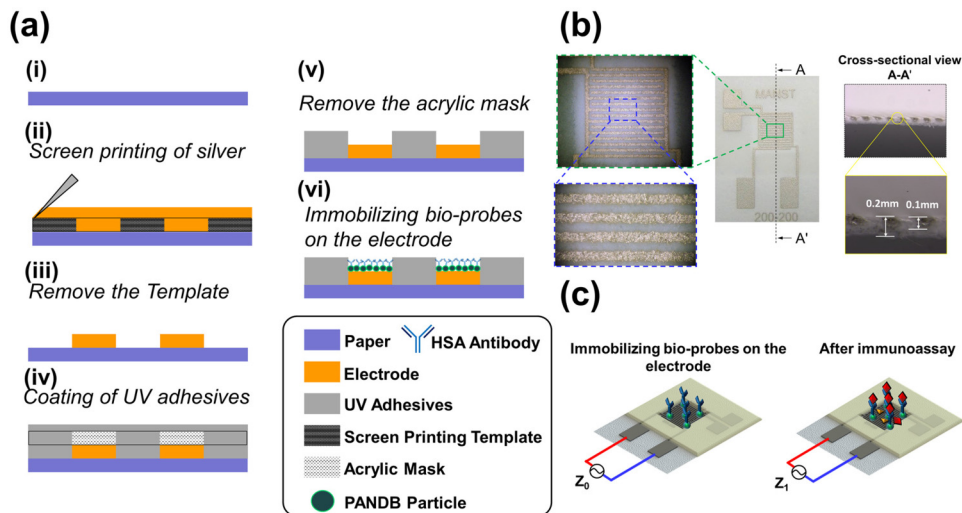


FIG. 3. (a) A schematic of the steps involved in the fabrication of the paper sensor. (b) An image of the completed sensor with enlarged optical microscopy images of the interdigitated microelectrodes. (c) Schematic of the paper sensor before and after immunosensing.

dropped on the filter paper using a plastic dropper and a glass stir rod is then used to evenly spread and penetrate the resin into the pores of the paper. Next, a PMMA mask is fabricated by laser cutting and shaded in black in certain areas to prevent UV light penetration. The mask is then aligned on the paper surface followed by exposure to a 400 W high-pressure mercury lamp (dominant wavelengths of 253 and 365 nm) for curing the resin. Finally, the paper is soaked in ethanol to remove the uncured resin followed by heating on a hotplate at 80 °C for 1 min to evaporate the remaining ethanol. The paper sensor is now ready for immobilization of microprobes, which are deposited on the hydrophilic sensing area using two methods:

1. Physical absorption

This method involves pipetting the microprobe solution on the hydrophilic sensing areas followed by quick drying using a suction assisted technique. As the $\text{Al}_2\text{O}_3/\text{PANI}/\text{ab-HSA}$ MPs are physically larger than the 1 μm filter paper pore size, they are retained on the sensing area surface and in effect form a thin film that covers the IDEs. 50 μl of $\text{Al}_2\text{O}_3/\text{PANI}$ MPs in DI water (1 wt. %) is pipetted on the sensing areas and the paper sensor is placed on a micro machined plastic device that is connected to a vacuum pump to enable effective drying within 10 min. After the MPs are trapped, the baseline impedance before immunosensing (Z_0) is recorded using an LCR meter (Wayne Kerr Electronics, WK 6420) in a frequency range of 20 Hz to 100 kHz at an applied voltage of 0.1 V. Next, 100 μl of DI water spiked with different concentrations of HSA protein were dropped onto the sensing areas and left for immunosensing for a further 30 min. This is followed by a washing step to remove any unbound proteins and the impedance after immunoassay is recorded (Z_1). The impedance measurements for each step (bare electrode, trapping, and immunosensing) were obtained in air. The impedance variation (ΔZ) during immunosensing can be mathematically expressed as $Z_1 - Z_0$. 10 immunosensors have been used to test each concentration of HSA and the error bars have been added. We have tried to eliminate any differences in initial impedance observed at different electrodes by normalizing the impedance response during immunosensing (ΔZ) with the initial impedance observed after microprobe trapping at that particular electrode (Z_0) and this is referred to as the normalized impedance variation ($\Delta Z/Z_0$). The normalized impedance variation is calculated at an operating frequency of 10 kHz for which we observe the maximum stable response during immunosensing. While a larger response can be observed at lower frequencies (<1 kHz), it shows lesser reproducibility and a lower signal-to-noise ratio as environmental conditions must be closely monitored and controlled while performing immunosensing.

2. Electrodeposition using p-DEP

This method utilizes DEP to trap the MPs specifically on the electrode surface as opposed to the entire sensing area. The sensitivity of impedimetric biosensors is strongly dependent on the bio-receptor immobilization strategy utilized. One of the aims of this study is to analyze if the immunosensor response is enhanced when MPs are trapped using DEP instead of physical absorption. The paper sensor is immersed in the microprobe solution and an AC signal of 10 V_{pp} at 1 kHz is applied for 10 min using a function generator (AFG3022, Tektronix) to trap the MPs based on the p-DEP force. We have chosen a frequency of 1 kHz since we observe the largest impedance change after microprobe trapping when using this frequency. The strength of the DEP force strongly depends on the medium and the electrical properties of the particles and their shape and size. Consequently, medium solutions with varying conductivity could be potentially for DEP immobilization, provided optimization of the applied signal frequency is performed. However, since we utilize p-DEP force (the particle attracted toward the region of the strong electrical field) for trapping the microprobes, a low conductivity medium like DI water is preferred so that the Clausius Mosotti factor is dominated by the dielectric properties of the microprobes and not the solution. After DEP trapping, all the steps are the same as that after physical absorption of microprobes as mentioned previously.

Besides DEP, other kinds of AC related electrokinetic forces such as AC electro-osmosis (ACEO) might also be present and effect microprobe manipulation. ACEO results in motion of

the liquid when an electrical potential is applied across a porous material or capillary tube like that present in cellulose paper. During application of an AC potential at a frequency of 1 kHz, ACEO may influence fluid movement within the pores of the filter paper between the IDE fingers. However, since the size of the microprobes used in this study is relatively large and they can only be trapped on the surface of the IDEs without being able to penetrate the filter paper, ACEO will not significantly influence microprobe trapping which should ideally be dominated by DEP.

III. RESULTS AND DISCUSSION

A. Physical absorption of MPs

The development of an electrical impedance based immunosensor requires effective immobilization of the antibodies on the electrode surface so that they can selectively capture the antigen, resulting in an impedance change. To enable sensitive and reproducible detection, the electrical pathway between the IDEs through the MPs and the captured antigen should be well defined. When the MPs are dropped onto the sensing area and immobilized via physical absorption, they form in effect a thin film on the surface of the IDEs. The electrical impedance of this film, which consists of semi-conductive polyaniline coated MPs, increases as the HSA protein is captured by the immobilized antibodies. As seen from the results, the normalized impedance variation gradually increases with an increasing concentration of HSA spiked DI water with an impedance variation of 0.65 that increases to 1.25 as the concentration increases from 0.375 mg/ml to 3 mg/ml. However, the repeatability of the observed variations was poor as highlighted by the wide error bars, which overlap for different concentrations. Since the MPs are not specifically immobilized on the IDE surface, the electrical pathway across the IDE fingers is random. Furthermore, physical immobilization results in movement or loss of MPs during the washing steps while cracks develop after drying as shown in Fig. 4(b), resulting in variations between different immunosensors and hence reduced reproducibility.

B. Dielectrophoretic trapping of MPs

The physical absorption approach poses challenges when the antibodies need to be immobilized specifically on the electrode surface. For impedimetric immunosensors utilizing IDEs, the

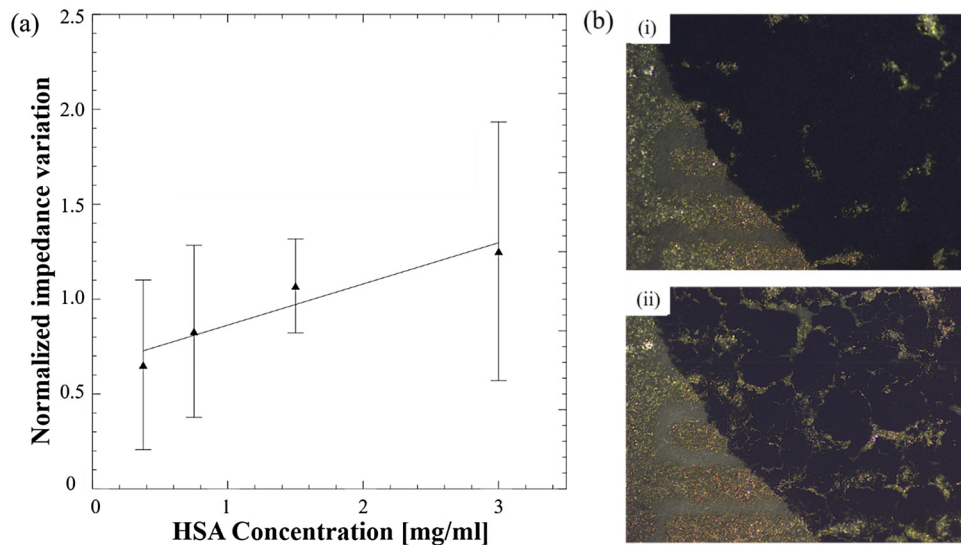


FIG. 4. (a) Normalized impedance variations for different concentrations of HSA using the physical absorption method for immobilizing MPs. (b) Optical microscopy image showing a layer of deposited MPs (i) before and (ii) after drying.

bioreceptor is generally immobilized either on the surface of the electrode or the gap in between. This ensures that the changes in electrical properties (resistance and capacitance) at the conductive electrode surface or the non-conductive gap are directly related to the immunoreaction. One way of improving physical immobilization on electrode surfaces is by using AC electrokinetic techniques like DEP to trap the MPs on the electrode surface. The optical microscopy images in Fig. 5(a) show that the MPs are successfully immobilized and uniformly adhere to the IDE surface when a positive dielectrophoretic force is applied. This ensures that the MPs remain firmly bound to the surface of the electrode after the washing step. Owing to the geometry of

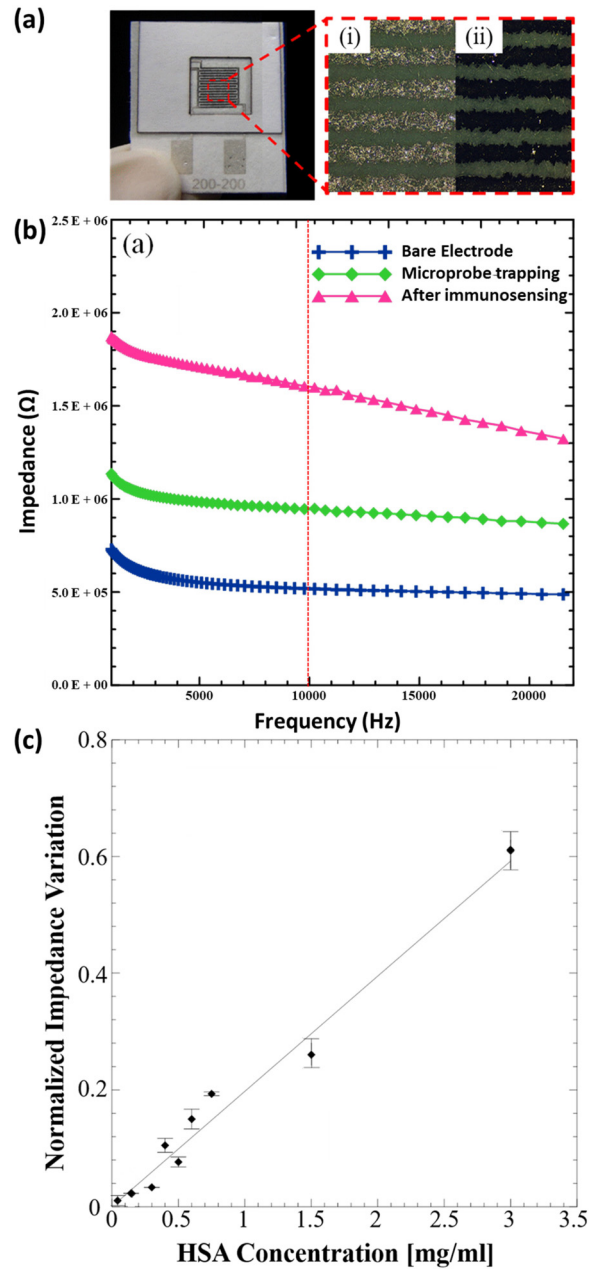


FIG. 5. (a) Image of the paper based immunosensor with the magnified area showing the silver microelectrode surface observed under an optical microscope (i) before and (ii) after trapping of MPs using p-DEP. (b) EIS spectra (bode plot) for each step during immunosensor fabrication and operation. (c) Normalized impedance variations for different concentrations of HSA.

IDEs, the current flow mainly occurs very close to the electrode surface, and the antibody-antigen complex formation directly impedes this flow when MPs are specifically trapped on the electrode using DEP. The impedance values obtained for each step (bare electrode, microprobe trapping, and after immunosensing) as a function of applied frequency are shown in the bode plot in Fig. 5(b). It can be seen that the impedance almost doubles at 10 kHz after microprobe trapping using p-DEP and further increases after immunosensing with the HSA protein (0.15 mg/ml). Since we measure the impedance change at a frequency of 10 kHz, capacitive effects should ideally dominate the impedance response. Both the microprobe trapping and the antigen binding can be envisioned as increasing the distance between the conducting plates of a capacitor which results in a decrease in the effective capacitance and consequently an increase in the overall impedance. It can be seen from the results in Fig 5(c) that the normalized impedance variation increases linearly over a wide range as the concentration of HSA in DI water increases from 50 $\mu\text{g/ml}$ to 3 mg/ml (linear regression equation is $Y = 0.19725 * X + 0.00028$ and $R^2 = 0.962645$). The limit of detection or LOD was observed to be 50 $\mu\text{g/ml}$, which is lower than that achieved using the physical absorption method. In addition, the immunosensor response shows significantly improved reproducibility and relatively lower variability in observed impedance response.

The proposed paper based immunoassay not only provides quantitative detection but also a lower LOD than the traditional urine dipstick, which displays a negative response under 100 $\mu\text{g/ml}$. However, in recent years, novel electrochemical biosensors fabricated on hydrophobic substrates and utilizing EIS transduction have been reported with significantly improved sensitivities.^{24–26} In our previous work, we fabricated a gold interdigitated microelectrode array on glass using a photolithographic protocol, which can detect bladder cancer biomarker Gal-1 with an achievable LOD in the pg/ml range.²⁷ Ding *et al.* reported an electrochemical immunosensor utilizing interdigitated electrodes fabricated on the silicon wafer and vertically aligned nanotube arrays capable of detecting oral cancer biomarker CIP2A in saliva with a limit of detection of 0.24 pg/ml range.²⁸ While several factors such as the ability to fabricate smaller microelectrode width and gap using photolithography result in lower LOD on hydrophobic surfaces, and there is also a fundamental difference in electrochemical measurements made on paper as compared to those performed in the free fluid on hydrophobic surfaces like glass. This is because the cellulose matrix prevents convection (in stationary fluids), acts as a barrier to diffusion (by increasing the tortuosity of the diffusion path), occupies some of the volume that would otherwise be occupied by fluid, and blocks a portion of the electrode surface ($\sim 30\%$, depending on the type of paper and fabrication method used).²⁹

Our aim in this research was to analyze the feasibility of fabricating a paper based immunosensing platform utilizing label free detection via EIS that could potentially be further improved to take advantages of paper, primarily its ability to wick fluids, to integrate complexity in assays like sequential fluid delivery. One of the key issues in fabricating label free affinity biosensors on paper is the selective immobilization of the affinity receptor such as antibodies or DNA on/in-between the interdigitated electrode fingers. Herein, we have shown that programmable DEP can be successfully used to trap microprobes selectively on the IDE surface, thus improving sensitivity and repeatability. To further reduce LOD, certain amplification strategies such as a sandwich immunoassay with a secondary antibody conjugated to a label (metal nanoparticles or enzymes) could be utilized. A sequential fluid delivery system can aid to integrate and automate these additional amplification steps, thus increasing suitability for point of care testing. Another challenge in developing paper based label free impedance immunosensors is the issue of specificity due to the non-specific absorption of a multitude of proteins present in clinical samples. While a washing step as performed in this study is helpful, it cannot guarantee the complete removal of physically absorbed proteins. A solution to this issue can be the use of differential analysis by fabricating a test (with antibody) and control (without antibody) site on the same immunosensor as shown below. Differential analysis (the ratio of normalized impedance variation at test and control sites) aids in eliminating non-specific binding effects and ensures that the impedance change after immunosensing is due to the formation of the antibody/antigen complex and not because of the physical immobilization of proteins.

IV. CONCLUSIONS

In summary, we have successfully demonstrated a proof-of-concept paper based electroanalytical platform that uses EIS for quantitative detection of immunoreactions. The combined use of interdigitated microelectrodes and dielectrophoretic trapping of MPs enabled improved sensitivity and reproducibility for label free immunosensing on paper. Future work involves the integration of this low cost, a disposable immunosensing platform with a portable impedance analyzer that can analyze and upload results to the cloud database as developed in our previous study,²⁶ which will enable effective point of care testing and improved public health monitoring. This proposed immunosensing platform could be extended to the development of a range of point of care affinity biosensors.

ACKNOWLEDGMENTS

The authors would like to thank the Ministry of Science and Technology, Taiwan, for financially supporting this research under Contract No. MOST 106-2632-E-218-001.

- ¹A. W. Martinez *et al.*, “Diagnostics for the developing world: Microfluidic paper-based analytical devices,” *Anal. Chem.* **82**, 3–10 (2009).
- ²A. W. Martinez, S. T. Phillips, and G. M. Whitesides, “Three-dimensional microfluidic devices fabricated in layered paper and tape,” *Proc. Natl. Acad. Sci.* **105**(50), 19606–19611 (2008).
- ³J. Yan *et al.*, “A microfluidic origami electrochemiluminescence aptamer-device based on a porous Au-paper electrode and a phenyleneethynylene derivative,” *Chem. Commun.* **49**(14), 1383–1385 (2013).
- ⁴E. Fu *et al.*, “Two-dimensional paper network format that enables simple multistep assays for use in low-resource settings in the context of malaria antigen detection,” *Anal. Chem.* **84**(10), 4574–4579 (2012).
- ⁵W. Dungchai, O. Chailapakul, and C. S. Henry, “Use of multiple colorimetric indicators for paper-based microfluidic devices,” *Anal. Chim. Acta* **674**(2), 227–233 (2010).
- ⁶M. Ploeg, K. K. Aben, and L. A. Kiemeny, “The present and future burden of urinary bladder cancer in the world,” *World J. Urol.* **27**(3), 289–293 (2009).
- ⁷J. S. Daniels and N. Pourmand, “Label-free impedance biosensors: Opportunities and challenges,” *Electroanalysis* **19**(12), 1239–1257 (2007).
- ⁸S.-J. Park, T. Andrew Taton, and C. A. Mirkin, “Array-based electrical detection of DNA with nanoparticle probes,” *Science* **295**(5559), 1503–1506 (2002).
- ⁹G. Zheng *et al.*, “Multiplexed electrical detection of cancer markers with nanowire sensor arrays,” *Nat. Biotechnol.* **23**(10), 1294–1301 (2005).
- ¹⁰B. V. Chikkaveeriah *et al.*, “Electrochemical immunosensors for detection of cancer protein biomarkers,” *ACS Nano* **6**(8), 6546–6561 (2012).
- ¹¹R. O. Dominguez, M. A. Alonso-Lomillo, and M. J. Arcos Martinez, “Recent developments in the field of screen-printed electrodes and their related applications,” *Talanta* **73**(2), 202–219 (2007).
- ¹²P. Labroo and Y. Cui, “Graphene nano-ink biosensor arrays on a microfluidic paper for multiplexed detection of metabolites,” *Anal. Chim. Acta* **813**, 90–96 (2014).
- ¹³F. Lisdat and D. Schäfer, “The use of electrochemical impedance spectroscopy for biosensing,” *Anal. Bioanal. Chem.* **391**(5), 1555 (2008).
- ¹⁴Y. Li, R. Afrasiabi, F. Fathi, N. Wang, C. Xiang, R. Love *et al.*, “Impedance based detection of pathogenic *E. coli* O157: H7 using a ferrocene-antimicrobial peptide modified biosensor,” *Biosens. Bioelectron.* **58**, 193–199 (2014).
- ¹⁵L. Das, S. Das, and J. Chatterjee, “Electrical bioimpedance analysis: A new method in cervical cancer screening,” *J. Med. Eng.* **2015**, 636075 (2015).
- ¹⁶R. Elshafey *et al.*, “Electrochemical impedance immunosensor based on gold nanoparticles–protein G for the detection of cancer marker epidermal growth factor receptor in human plasma and brain tissue,” *Biosens. Bioelectron.* **50**, 143–149 (2013).
- ¹⁷C. Zhang *et al.*, “Dielectrophoresis for manipulation of micro/nano particles in microfluidic systems,” *Anal. Bioanal. Chem.* **396**(1), 401–420 (2010).
- ¹⁸H. A. Pohl, “The motion and precipitation of suspensions in divergent electric fields,” *J. Appl. Phys.* **22**(7), 869–871 (1951).
- ¹⁹V. Nhan, “Lab on a chip for multiplexed immunoassays to detect bladder cancer using multifunctional dielectrophoretic manipulations,” *Lab Chip* **15**(14), 3056–3064 (2015).
- ²⁰M. S. Harrington and L. B. Anderson, “Analytical strategies using interdigitated filar microelectrodes,” *Anal. Chem.* **62**(6), 546–550 (1990).
- ²¹V. Guarino *et al.*, “Electro-Active Polymers (EAPs): A promising route to design bio-organic/bioinspired platforms with on demand functionalities,” *Polymers* **8**(5), 185 (2016).
- ²²B. Belaabed *et al.*, “Polyaniline-doped benzene sulfonic acid/epoxy resin composites: Structural, morphological, thermal and dielectric behaviors,” *Polym. J.* **42**(7), 546–554 (2010).
- ²³N. Prabhakar, Z. Matharu, and B. D. Malhotra, “Polyaniline Langmuir–Blodgett film based aptasensor for ochratoxin A detection,” *Biosens. Bioelectron.* **26**(10), 4006–4011 (2011).
- ²⁴A. R. Mahon *et al.*, “Molecular detection of invasive species in heterogeneous mixtures using a microfluidic carbon nanotube platform,” *PLoS ONE* **6**(2), e17280 (2011).

- ²⁵S. Basuray *et al.*, “Shear and AC field enhanced carbon nanotube impedance assay for rapid, sensitive, and mismatch-discriminating DNA hybridization,” *ACS Nano* **3**(7), 1823–1830 (2009).
- ²⁶D. Li *et al.*, “A shear-enhanced CNT-assembly nanosensor platform for ultra-sensitive and selective protein detection,” *Biosens. Bioelectron.* **97**, 143–149 (2017).
- ²⁷C.-H. Chuang *et al.*, “Immunosensor for the ultrasensitive and quantitative detection of bladder cancer in point of care testing,” *Biosens. Bioelectron.* **84**, 126–132 (2016).
- ²⁸S. Ding *et al.*, “CIP2A immunosensor comprised of vertically-aligned carbon nanotube interdigitated electrodes towards point-of-care oral cancer screening,” *Biosens. Bioelectron.* **117**, 68–74 (2018).
- ²⁹E. J. Maxwell, A. D. Mazzeo, and G. M. Whitesides, “Paper-based electroanalytical devices for accessible diagnostic testing,” *MRS Bull.* **38**(04), 309–314 (2013).